Turk J Phys
32 (2008) , 65 – 77.

Effects of Opacity on Stellar Radii and Their Relevance to Observational Data

Gülay İNLEK[1], Aysun BÖKE[1], Oktay YILMAZ[2], Edwin BUDDING[2,3]
[1] *Physics Department, Balıkesir University, Çağış Campus, 10145, Balıkesir-TURKEY*
[2] *Physics Department, Çanakkale Onsekiz Mart University, 17100 Çanakkale-TURKEY*
[3] *Carter Observatory, PO Box 2909, Wellington-NEW ZEALAND*

Received 31.12.2007

Abstract

We have examined the effect of varying opacities on envelope structure with the aid of Paczyński's public domain stellar modelling programs. For this, we prepared new opacity tables from the data of Kurucz [1], using Lagrange interpolation to obtain the tabular values. We compare the results of these Kurucz opacities with similar tabulations from Huebner et al. [2], Iglesias and Rogers [3], Rogers and Iglesias [4] and Iglesias and Rogers [5]. We have checked calculations for the same ranges of stars considered originally by Schwarzschild [6], and compared our findings, using newer opacity data, with those of other sources. We consider how such calculations relate to high accuracy observational data, with the well-observed planetary eclipsing system V 376 Peg (HD 209458), providing a guideline towards data of similar accuracy in the near future. Current accuracies on absolute radii and masses derivable from eclipsing spectroscopic binaries are conservatively estimated at ∼1%. The effects of revised opacity calculations on the radii of stars of intermediate mass are several times greater than this (5–10% for constant values of other parameters), so that eclipsing binary data should have good potential for independent tests of opacity theory across a wide range of stellar types.

Key Words: Stars: general-structure: modelling, opacity tables, observational tests, eclipsing binary data

1. Introduction

While many studies show that radiative transport plays a key role in shaping the structure and evolution of stars, no direct measurements of the opacity of matter to radiation in stellar interiors are possible. Theoretical calculations are required if a star's internal conditions are to be interpreted. Over the years, various opacity formulae and tables have been applied to structural models. In his seminal book, *The Structure and Evolution of the Stars*, Schwarzschild discussed effects associated with the ionization of different atomic species, i.e. bound-free transitions, free-free absorption and electron scattering [6]. The net effects of bound-bound (line) absorptions subsequently received closer attention, and have been shown to make a significant contribution [7, 5, 1]. Schwarzschild also compared theoretical models with results from the observations of binary stars. This approach to checking models was supported by Strömgren [8] and many subsequent authors.

Opacity appears in the radiative transfer equation of stellar structure [9], which can be put in a form such as

$$\frac{dK}{dr} = -\kappa\rho H = -\kappa\rho L/16\pi r^2, \tag{1}$$

where K and H are the Eddington radiation pressure and flux terms, respectively, and L is the global luminosity, coming from the separate energy generation equation (all functions of the radius r, as are the

local density ρ and temperature T). K is given in the internal regions, to high accuracy by

$$K = \frac{\sigma T^4}{3}, \tag{2}$$

where σ is Stefan's constant. The opacity thus relates the total heat flow to the local temperature gradient, the latter being greater in regions of greater local opacity. In averaging over all frequencies, the 'Rosseland mean' opacity, $\kappa \equiv \kappa_R$, yields a temperature gradient form of the transfer equation; thus

$$\left(\frac{\sigma T^3}{\kappa_R}\right)\frac{dT}{dr} = -\frac{3\rho L}{64\pi r^2}, \tag{3}$$

since the Rosseland mean is defined by

$$\frac{\sigma T^3}{\kappa_R} = \pi \int_0^\infty \frac{1}{\kappa_\nu}\frac{dB_\nu(T)}{dT}d\nu. \tag{4}$$

Rosseland mean opacities κ_R (in units of $\mathrm{cm^2 g^{-1}}$) therefore weight the effect of frequency in proportion to the flux contribution at that frequency. In a more general context, we should consider other contributions than radiative transparency (inverse of opacity) to the total flow of heat, particularly electron conductivity [10], but in this article we concentrate only on the effects of radiative transfer. We especially seek to clarify the extent to which observational data on representative stars can test theory on this.

It is feasible, in a general way, that the radiative opacity of the plasma in stellar interiors may tend to idealized forms in certain limiting conditions. For example, we could anticipate that a totally ionized hydrogen medium, characterized only by free-free transitions, would have a transparency component proportional to the radiative energy density per unit material density. But, in traversing a layer of such a medium, the outward flux receives a contribution proportional to the linear velocity of the electrons, associated with the decrease of the Debye screening length. From such a view, a form such as

$$\kappa \propto \rho T^{-7/2} \tag{5}$$

(Kramers' law) appears reasonable [6]. Similarly, another limit, that of Thomson scattering by electrons ($\log \kappa \sim -0.47$), should take over in fairly high temperature (but not too high density) plasma conditions when the foregoing formula gives low enough opacity values [6].

More generally, we can expect the net opacity to be dependent of the (varying) composition, initially set by the fractional proportions of hydrogen X, helium Y and other atoms Z (= metallicity), where $X + Y + Z = 1$, as well as ρ and T, i.e. $\kappa_\nu = \kappa_\nu(X, Z, \rho, T)$. The nature of this dependence, in detail, involves modelling the way electromagnetic waves interact with the local field configurations around the plasma's constituent particles. Procedures have developed from the early Thomas-Fermi treatment towards long and complex calculations that have become the reserve of certain patient specialists; a point made in the review of Carson [11]. Carson also noted that the results of separately published calculations of apparently similar situations did not always agree with each other (within factors of the order of unity). Moreover, the necessity to use both physical and mathematical approximations to describe the inherently complex interactions implies that such calculations cannot be regarded as a closed subject. The onward progress of computational capabilities should allow continued advances in the modelling of absorption and consequently stellar structure.

For practical applications in astrophysics, tables of representative opacity values are generally presented in two-dimensional format (for $\log \rho$ and $\log T$, given the large variation of density and temperature and the regular use of variables in logarithmic form), with selected values of X and Z. Since there is, in most stars, a strong correlation between the runs of density and temperature values ($\rho \sim T^3$), the variable $\mathcal{R}$ was introduced for convenient general tabulation [3], where

$$\log \mathcal{R} = \log \rho - 3 \log T + 18. \tag{6}$$

In our present study we have applied opacity tables that originated in the work of Cox and Stewart [12] at Los Alamos National Laboratory (as modified by later authors); Iglesias and Rogers [3], Rogers and Iglesias [4], Iglesias and Rogers [5] and Kurucz [1], to the stellar model code GOB [13]. We have discussed previously

how we used and checked this program [14] and we say more about its use in the following subsection. It is well-known that opacity effects are strongest in the outer parts of the star where the temperature gradient steepens as the major constituent elements start to recombine [15] . This is predominantly in the regions dealt with by GOB. It was necessary to tailor published opacities [1] to the format required by GOB and to do this we used four point Lagrange interpolation. We thus calculated κ for the required 31 values of log density in the range of –12 to +3 in steps of 0.5 and 51 values of log temperature from 3.25 in steps of 0.075. We discuss more about this in section 2 and in section 3 present the results of different opacity tables in the outputs of the programs GOB and also SCH, a second modelling program that deals with the bulk of the stellar mass [13].

While we cannot measure internal opacities directly, the possibility to check different sets of calculations from resultant models of stars is challenging. There are various options about this, but our present study addresses the data on eclipsing binary systems. Nowadays, such data are entering a new phase of very high accuracy [16], stimulated, in part, by the search for new planetary systems. The prototype V 376 Peg (HD 209458) has attained particular significance in this regard, and while the extraordinary accuracy of HST photometry is not expected to be available in a wholesale way, it provides guidelines not only for future space-based photometry, but also for well-selected terrestrial facilities. On that point, we examine the milli-magnitude accuracy light curve of the primary transit of V 376 Peg by [17], as observed at Mauna Kea. We combine 3 data sets of [17] and discuss how such results relate to stellar modelling in section 4.

Of course, other things than opacity affect the measured parameters of observed stars, the overall mass usually being regarded as the first determinant of these. The positions of stars of given masses in colour-magnitude diagrams have then been usually related to evolutionary effects. Evolutionary paths, as well as their starting positions, are themselves different in dependence on the composition of the stellar material [18]. The main question for our present study, however, is what precision of observational results would allow alternative models for the opacities through the envelope, to be effectively discriminated. Andersen et al. proposed that parameter estimation errors should be no larger that about 1% in the radius, and 2% in the mass and temperature, to enable useful checks on opacities; this for stars whose metallicity can be assigned to within about 25% of its real value [19]. Coevally formed eclipsing spectrographic binaries, whose components have not had significant interactive evolution, should permit isochronal tests of theory in which some of the indeterminacy is removed, as noted by Strömgren [8]. Andersen [20], and other authors in similar programmes, have thus used high quality observational data of such binaries to test modelling. A recent discussion was that of Claret [21]. Persistent differences between older models and data led to further theoretical inferences, for example regarding more generalized versions of the treatment of convection [22, 23]. But opacity theory itself has not been static, and various new sets of calculations were published since the early nineties. A summary discussion (section 5) comments on the interplay between data-analysis and the results of theoretical modelling, and implications for both activities.

1.1. Use of the programs GOB and SCH in model construction

It is well-known that the construction of a simple stellar model in one spatial dimension reduces, generally, to a two-point boundary value problem involving the (numerical) quadrature of 4 simultaneous linear first-order differential equations (cf. e.g. Schwarzschild [6]. A short introduction to the programs discussed in this paper is given by [24]; demonstration versions have also been produced by Odell [25]).

Regarding the imposed boundary conditions: the inner boundary is conceptually simpler. The independent variable, normally the internal mass M_r, is here zero, along with the radius r and luminosity L_r. The boundary values of central temperature and density, T_c and ρ_c, are assigned preliminary estimates, so the quadrature can proceed to some internal point, where the outward integration will be matched with the inward one from the outer boundary.

The outer boundary is more complicated for various reasons. One is that a main aim in the 'solution' of the modelling problem is to relate observational results to the two outer boundary values determined by a self-consistent quadrature. Normally, two quantities that can be directly matched to measurements are the surface luminosity L_0 and effective temperature T_e. The structure equations themselves should primarily specify L_0 and R, as paired opposites to the central density and temperature (the inner boundary); but since R can be expressed as $R = \sqrt{L_0/4\pi\sigma T_e^4}$, it appears this point can be dealt with, although the R in

question should really be that at the actual outer 'boundary' of the star (at a slightly different radius), where the density ρ_0 becomes formally zero. Note that a separate relation connecting T_e to the boundary layer temperature T_0 comes from model atmosphere theory [14]. Another point is that, in these outer layers, the problem has degenerated to one involving only 3 variables, since L_0 settles to an essentially constant value outside the central energy-generating regions.

The program GOB (generates the outer boundary) is intended to take care of these issues. The program constructs a set of model atmospheres for four corner points in the L_0, T_0 plane that should enclose the true final values resulting from a self-consistent complete model. The GOB inward integration proceeds, in principle, down to a user-set base-of-atmosphere layer $M_r = M_B$, which is typically $0.95 \times M_R$, the total mass of the star. In practice, some control parameters intervene if the temperature becomes too high or the number of integration steps unmanageably large. Since there are only 3 differential equations to integrate and no match-point fitting, this program proceeds quickly. At the lower boundary GOB produces a set of ρ_B, T_B and R_B values, with $L_0 = L_B$ also holding valid. Given these 4 corner values, it is possible to make (linear) interpolations for intermediate points to find base of atmosphere values. We can thus write, for a base density corresponding to a general surface point L_0, R, say (R being derived from the assigned T_e)

$$\begin{aligned}\rho_B(L_0, R) &= \rho_B(L_1, R_1) + \frac{L_0 - L_1}{L_2 - L_1}[\rho_B(L_2, R_1) - \rho_B(L_1, R_1)] + \\ &+ \frac{R - R_1}{R_2 - R_1}[\rho_B(L_1, R_2) - \rho_B(L_1, R_1)]. \end{aligned} \quad (7)$$

The 4 base values for such surface L_{0i}, T_{0j} pairs, enclosing a particular trial L_0, R pair, are given, together with the trial pair itself, by GOB as input for the inward integration in SCH. The outward integration from the centre is compared with the inward integration from this $0.95M_R$ level at a selected inner fitting point, which is typically $M_r = M_R/2$. The averages of the 4 pairs of variables at this fitting point are taken as new starting values for backward integrations to the boundaries, and an iteration process thus started.

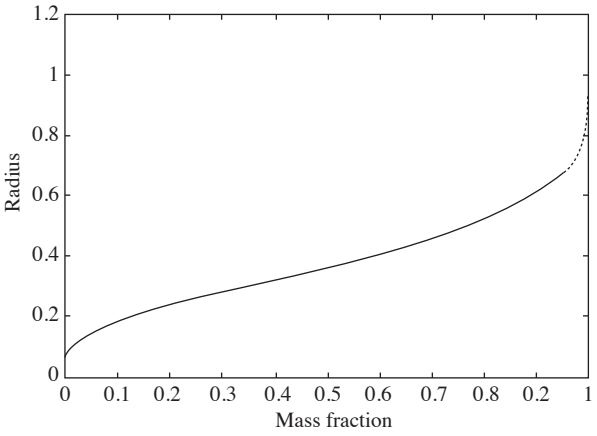

Figure 1. Combination of SCH and GOB integrations for the radial variation with mass of a zero-age 1 solar mass model.

It is easy to visualize new central values of T_c and ρ_c being substituted back in a second outward run from the centre. At the outer boundary of the SCH run, however, there will be new values for all four variables; but it is really only the L_0 and R surface pair that are independently corrected by the integrations of this two-point problem. The new surface L_0 is obtained directly, since it does not vary through the outer layers. The corresponding new surface value of R can be derived, using the new L_0 and the original GOB surface values R_1 and R_2, for which corresponding values of R_{B1}, R_{B2} are known. These $R_{B1,2}$ values are compared with the R_B newly obtained from the outward integration. A corresponding corrected surface value of R may then be interpolated. Having the new surface values of L_0 and R allows a new set of base values to be obtained, with ρ and T starting values derived from equation (7) (for ρ_B, with a corresponding equation for T_B) for a second, corrected, inward integration. In a convergent problem, the differences between the four

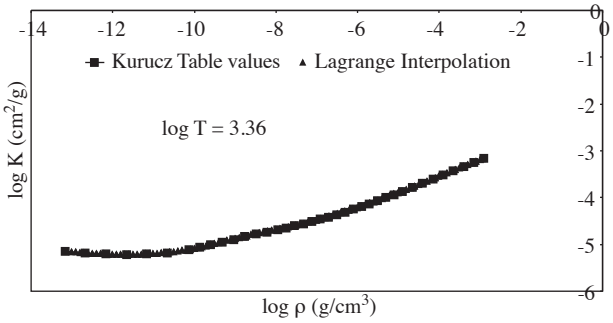

Figure 2. Example of Lagrange-interpolation through Kurucz tabulated opacities.

pairs of variables at the inner matching point become progressively less and the sequence is terminated when these differences pass below some set accuracy control limit. Convergence is normally found in practice, if the starting values are not too far from the final ones. Initial errors of more than 20 percent in the logarithms of trial parameters may cause lack of convergence. Figure 1 shows that there is a good agreement between SCH and GOB integrations.

2. Opacity Tables

We require interpolations in the two dimensions of (log) temperature and (log) density for given (log) opacities for a fixed chemical composition: so we first interpolated $\log \kappa_R$ for different $\log \rho$ values at constant temperature and then interpolated for the log temperatures with $\log \rho$ at each tabular value. Figure 2 shows such Lagrange interpolated points passing smoothly through the Kurucz [1] tabular values.

The Kurucz [1] model atmosphere program, whose results we have used, includes more than 1000 atomic and molecular species, each having up to 10 isotopic forms. It deals in detail with the ions of all elements up to zinc. This modelling has improved opacity values particularly from including such a large number of atomic species, especially accounting for the net effect of their line (bound-bound) absorptions [26]. There are three aspects to this. The first involves direct calculation of the spectrum at given pressure and temperature to include more than 10^8 separate lines. This involves a wavelength resolution high enough to resolve natural spectral features smaller than observed widths associated with the Doppler effect in thermal and rotational motions. Another aspect of the modelling involves tabulating statistical distribution functions for the line opacities in dependence on temperature and pressure over suitably wide ranges of values for various assigned abundances. The third aspect is the spectral sampling, using a relatively small number of wavelength points that do not resolve the spectrum in detail. In computing an atmospheric model, the relevant quantity of interest is a spectral integral, where detailed broadening effects have been smoothed out. This is referred to as 'opacity sampling'. The twelfth edition of the program ATLAS [27] computes Rosseland mean opacities at given temperatures and densities using iterative procedures incorporating these three procedures.

Iglesias and Rogers constructed the OPAL code to calculate Rosseland mean opacities [3]. They gave extensive results for the mixture of [28], which allow accurate interpolation in (log) temperature and density, with given hydrogen with various metal mass fractions. They used temperature as the basic variable and also $\mathcal{R} \propto$ density/(temperature)^3 (see above). The range of $\mathcal{R}$ and temperature are such as to cover typical stellar conditions from the interior through the envelope to extended outer regions. Iglesias and Rogers did not review cool atmospheres, because, at that time, they were unable to revise photoabsorption by molecules [3]. Only radiative processes were taken into account, so that electron conduction was also neglected. Their approach regarded distant many-particle correlations as highly classical, and their detailed radiative interaction calculations were applied to regions where the de Broglie wavelength is less than the plasma screening length. Here, they introduced systematic quantum mechanical methods for many-particle correlations. Their model calculations are generally accepted to be accurate, both for valence electrons and photon absorptions involving inner core electrons, as well as multiply excited ions. Bound-bound transitions were calculated for every subshell in each configuration of the various ion stages explicitly.

The Cox and Stewart [12] opacity tables, sometimes known as the (older) Los Alamos data, presented Rosseland mean opacities also without allowance for electron conduction. These tables have provided a basis for many stellar structure calculations, including the original GOB program. They include molecular-hydrogen and free-electron absorption of radiation by the free-free process from [29]. Rayleigh scattering of photons by molecular hydrogen, using a formula given by [30] was also included. The older Los Alamos tables were presented in an updated form by [2] (the Los Alamos Opacity Library – LAOL), and in this form appeared in the original versions of the Paczyński code available to our group.

Creation of full two-dimensional interpolated tables needed for GOB involves a two-step procedure: first interpolating density values from the source (in their format) to the required (GOB) table format, e.g. first for the required densities at set temperatures. These opacities are then interpolated to the required temperatures at the new tabular densities.

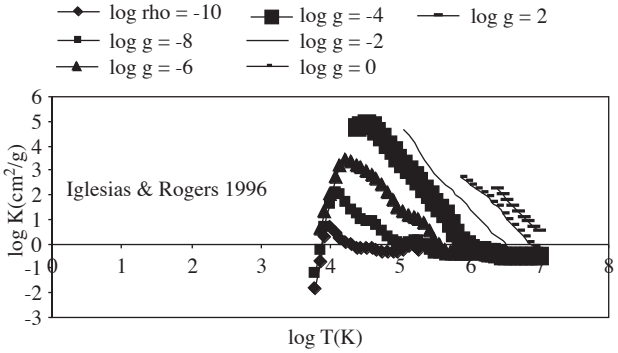

Figure 3. Iglesias and Rogers (1996) opacity values (in cm^2 g^{-1}), for $X = 0.70$, $Y = 0.27$, $Z = 0.03$, with changing temperatures at different densities.

The inset in Figure 3 shows the density values for each run of opacities. The high density region, to the right of the opacity peak, shows reversion to a Kramers' type form. This seems most clear for the log $\rho = -4$ curve. This declines to the simple electron scattering constant form ($\kappa \sim$ constant) for high temperatures. At the low density side, there is the expected decline to very low opacities near the surface. Peak values of the opacity in the tables occur at about log $\rho \sim -2.5$ and log $T \sim 4.5$ and are typically around log $\kappa \sim 5.5$. Newer opacity calculations show this peak occurring at somewhat lower temperatures than the older tables.

Figure 4 shows three dimensional presentation of different opacity tables we have used in GOB programme.

It can be seen that the Iglesias and Rogers opacities are basically similar to the LAOL ones, except in the outer parts of the atmosphere where densities and temperatures are low. The Kurucz [1] opacities also show differences in the outer envelope. This can be associated with the more detailed treatment of line absorptions by Kurucz. Our presentation reflects some discontinuity towards the higher densities and temperatures for the Kurucz opacities. This is because the available tabulations did not cover the complete ranges of variables required for all feasible stellar conditions, but they are sufficient for the important outer ranges of the envelope.

3. Results of Different Opacities in Model Integrations

Schwarzschild's book [6] considered 10, 5 and 2.5 solar mass models (at zero age), and for the lower Main Sequence, 1 and 0.6 solar masses. We follow the same selection in Table 1, where corresponding SCH output boundary radii, luminosities and effective temperatures have been tabulated in Table 1(c) for comparison. We also list GOB base-of-atmosphere radii corresponding to these luminosities and effective temperatures. Three sub-tables are given corresponding to a selectable (mean) interpolation step used in the numerical integration of the outer envelope. Actually, there are separate interpolation step limits set for each of the main structural variables, and that for log ρ, for example, will be greater than that for log T, given the range of variation of the corresponding values. The values shown, however, represent a user-set control over the

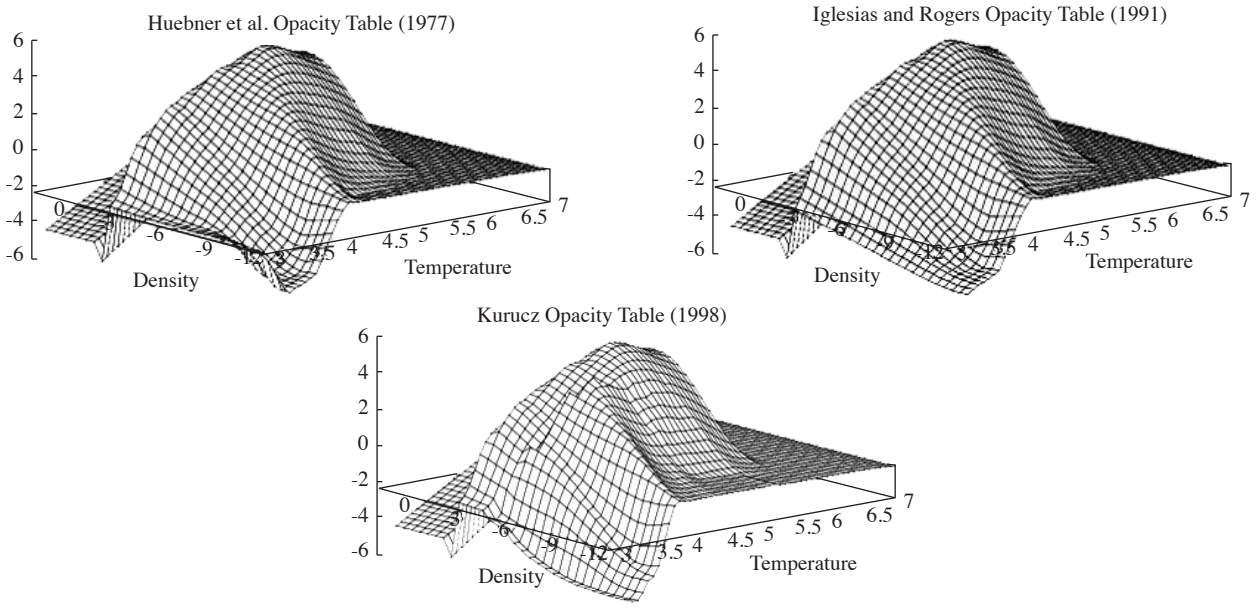

Figure 4. Three-dimensional representation of opacity tables: (a) Huebner et al. (1977); (b) Iglesias and Rogers (1991); and (c) Kurucz (1998).

inherent accuracy of the quadrature. There appears no exact basis for the selection of this control. In some regions, the underlying variables are changing relatively slowly and the cumulative effects of departures from linearity over small integration steps should be small, perhaps even self-cancelling. It is in the regions close to absorption edges, where changes are rapid and non-linear, that opacity calculations are most difficult. Twenty percent differences between the opacities of different sources, together with admitted theoretical uncertainties of this order, imply that decreasing the interpolation steps to very small values cannot increase the inherent accuracy of the model. We have presented the subtables in order to view the effect of the selected interpolation step size in relation to the scale of effects from different opacity tables.

It is clear from Table 1 that the significantly greater opacities in the outer layers of the models increases the corresponding temperature gradient in these layers, as can be anticipated from equation (3). The tables show that the differences between corresponding base layer values of the variables resulting from the different opacity tables are re of the order several percent (of their values). It is noticeable, however, that these differences are comparable to numerical effects in the way the integration may be performed in relation to step sizes. A similar point was made by Stothers [31].

The base values in Table 1 result from inward integrations with different opacities, but from the same outer boundary. For a complete model, the atmospheric base and perimeter of the SCH integration values should join up, as indicated in Figure 1, although this requires some adjustment of the outer boundary temperature. What happens when more recent, increased, opacities are put into the GOB program is that the base layer temperature increases and locates itself further out in the envelope. If the original GOB and SCH integrations had matched at the base layer, therefore, we would have to decrease the value of T_0 for the GOB integration with the new opacities (at given luminosity) to achieve the same base temperature. This decrease of T_0 for constant L means that the effective radius of the star should expand [7]. The proportional effect is of the same order as the proportional changes to the base temperatures for small changes, i.e. 5–10 %. Calculated radial changes produced in this way for the examples given are also provided in Table 1.

From Stothers and Chin [32] it follows that about the same increase in radius (5–10%) between the older [12] and newer [2] Los Alamos opacities is given by a 50% increase in metallicity. We did not study changes of metallicity for the present work, but Stothers and Chin's finding is in keeping with Andersen's [20] point that if the metallicity can be correctly assigned to within 25%, and we know the age of the star (i.e. its probable evolution), then it should be possible independently to check the effects of opacity. In this connection, it is interesting that this scale of radial increase (5-10% – for intermediate-low mass stars) was

Table 1. GOB and SCH results for base layer radii using different opacity tables: (a) for mean interpolation step = 0.1; (b) for step size = 0.05; and (c) for step size = 0.02.

(a) Parameter	Value				
$M_\odot$	0.60	1	2.5	5	10
R_B (Huebner)	0.3287	0.4886	0.982	1.7216	2.3481
R_B (Igl. 1991)	0.3287	0.4886	0.982	1.7216	2.3481
R_B (Igl. 1996)	0.3589	0.5318	1.0656	1.8286	2.4540
R_B (Kurucz)	0.3529	0.5263	1.0231	1.7311	2.3575
$\log L$	–0.8276	0.0409	1.6068	2.8296	3.6749
$\log T_e$	3.652	3.7692	4.0115	4.2085	4.3545
R (OB Huebner)	0.5680	0.6131	1.127	1.966	3.349
R (OB Igl. 1991)	0.5680	0.6131	1.127	1.966	3.349
R (OB Igl. 1996)	0.6335	0.6896	1.719	2.527	3.418
R (OB Kurucz)	0.598	0.6232	1.714	2.316	3.401

(b) Parameter	Value				
$M_\odot$	0.6	1	2.5	5	10
R_B (Huebner)	0.3741	0.5523	1.0300	1.7317	2.3565
R_B (Igl. 1991)	0.3741	0.5523	1.0300	1.7317	2.3565
R_B (Igl. 1996)	0.3805	0.5592	1.1092	1.8317	2.4610
R_B (Kurucz)	0.3742	0.5459	1.0384	1.7423	2.3604
$\log L$	–0.8276	0.0409	1.6068	2.8296	3.6749
$\log T_e$	3.652	3.7692	4.0115	4.2085	4.3545
R (OB Huebner)	0.5736	0.6301	1.166	1.968	3.389
R (OB Igl. 1991)	0.5736	0.6301	1.166	1.968	3.389
R (OB Igl. 1996)	0.6414	0.7380	1.879	2.638	3.926
R (OB Kurucz)	0.6398	0.7221	1.792	2.413	3.517

(c) Parameter	Value				
$M_\odot$	0.6	1	2.5	5	10
R_B (Huebner)	0.3871	0.5733	1.1357	1.8710	2.5258
R_B (Igl. 1991)	0.3871	0.5733	1.1357	1.8710	2.5258
R_B (Igl. 1996)	0.3869	0.5728	1.1379	1.8755	2.5345
R_B (Kurucz)	0.3869	0.5728	1.1381	1.8768	2.5340
$\log L$	–0.8276	0.0409	1.6068	2.8296	3.6749
$\log T_e$	3.652	3.7692	4.0115	4.2085	4.3545
R (OB Sch. 1958)	0.644	1.021	1.591	2.381	3.622
R (OB Huebner)	0.6484	0.6998	1.176	1.978	3.457
R (OB Igl. 1991)	0.6484	0.6998	1.176	1.978	3.457
R (OB Igl. 1996)	0.6716	0.7590	1.963	2.736	3.996
R (OB Kurucz)	0.6511	0.7988	1.896	2.517	3.687

sufficient to resolve remaining apparent discrepencies between observations and theory, according to Stothers and Chin [32] (given appropriate masses[33]). In Table 2 we present results for these radial increases as given by Stothers and Chin [32] and also Claret and Gimenez [34].

A key question is whether the measured values of luminosity and effective temperature, at given mass and (surface) composition, are sufficient uniquely to resolve the internal run of all parameters affecting the heat flow (in particular, radiative opacities) as well as the age. It has been argued by [21] that, given detached eclipsing binaries with separately measurable radial velocities and no interactive evolution, the age can be

Table 2. Comparison of radial increases associated with increase in opacity.

(a) Parameter			Value		
$M_{\odot}$	0.6	1	2.5	5	10
S & C (1991)	—	—	0.10	0.07	0.05
C & G (1992)	—	—	0.08	0.07	0.10
Present	0.092	0.088	0.085	0.062	0.045

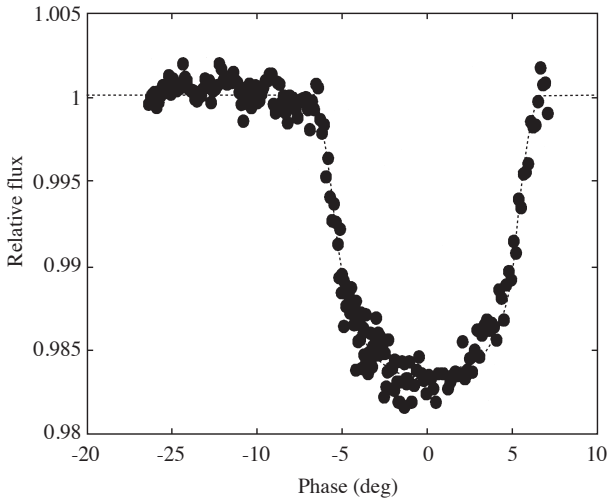

Figure 5. B light curve combining data from three transits across the disk of V376 Peg by its 'planetary' companion as observed by Sullivan and Sullivan (2003).

effectively eliminated by combining one pair of measures (luminosities, say), leaving the other pair (e.g. ratio of effective temperatures) to fix the heat-flow regime. But since approximations used in the calculations of opacities are in a process of steady refinement, this question cannot be regarded as having a fixed answer, although at any particular time the latest models can be tested.

4. Observational Tests

It is well-known that, regarding the properties of pulsating stars, the opacity distribution has a sensitive relationship to behaviour [35]). But applications of data on eclipsing binary stars to general tests of theory have also been discussed, at least since H.N. Russell's [36] centennial symposium on the 'Royal Road' to determine absolute stellar properties, and with much more precision available in recent years. The coeval origin of binary stars also offers special convenience, as mentioned before.

A significant part of our present article is to assess how well currently available data are able to relate to the results of improved opacity tabulations. We have selected V376 Peg = HD 209458 as an interesting test case. In Figure 5, B photometry of the 'planetary' transits in this system observed from Hawaii in 1999 and 2000 have been combined and shown together with an optimal curve fit. Background information about these observations was given by [37]. HD 209458 was one of a small number of selected stars showing spectral evidence of low mass companions with reasonably short periods, some proportion of which would be likely to show eclipses [38]). These particular data were considered previously, as individual light curves, by Budding [39].

The data in Figure 5 were analysed using the CURVEFIT package [40]. The fitting function in this package comes from an approximate solution, using spherical harmonics, to the underlying Poisson equation for the distortion of figure caused by tidal interactions and rotation, along classical lines. Speed of evaluation

of an algebraic form of fitting function is an advantage when exploring a wide range of parameter space and evaluating the corresponding error matrix. That this matrix corresponds, geometrically, to a closed ellipsoid is sufficient and necessary for formal determinacy of the underlying model. The properties of the error matrix allow us to check that the parametrization neither surpasses nor under-utilizes the information content of the data (hence the general name 'information limit optimization technique' (ILOT) cf., e.g. Banks and Budding [41]). Initial guidelines for the parameters of V376 Peg were taken from [42] and [17].

Table 3. V376 Peg (a) curve-fit details: optimal parameters and errors; (b) absolute parameters.

(a) Parameter	Value	Err. (σ)
U	1.0012	0.0009
r_1	0.1172	0.001
r_2	0.0145	0.0006
i	86.3	0.4
u	0.574	
$\Delta l'$	0.001	
χ^2/ν	0.93	

(b) Parameter	Value	p.e.
Period	3.52474 d	0.00001 d
Epoch (HJD)	2451497.7993	
A	9.837	0.04 $R_\odot$
R_1	1.15	0.01 $R_\odot$
R_2	1.39	0.03 R_{Jup}
i	86.3	0.3 deg
u	0.57	0.14
M_1	1.03 $M_\odot$	*
M_2	0.62 M_{Jup}	*
V_{Abs}	4.31	
V	7.653	*
B–V	0.594	*
T	5920 K	
Dist.	46.7	0.8 pc

* cf. Henry et al. 2000

CURVEFIT provides radii, in terms of the separation of the component stars, as well as the orbital inclination, from the eclipse photometry. Results are given in the upper part of Table 3. These parameters can be combined with the high quality radial velocity data of [42]. Since the projected velocities are measured in absolute units (e.g. km·sec^{-1}) and the orbital period is known independently, the orbital radius can be deduced in km. Kepler's law will then furnish the masses of the components. In this way we calculated the absolute radii in the lower part of Table 3. From the goodness of fit measure χ^2, the stellar radius is estimated probably to within 1 percent of its true value.

The results given in Table 3 are within their error limits of those of Brown et al. [43], using the much more sophisticated facilities of the Hubble Space Telescope. They are a thus a fair indication of generally available good observational accuracy of the present time, when sufficient precautions are taken. It is worth noting that the ∼millimag accuracy presented by [17] was achievable even with a 0.6 m telescope and 2 min integrations from a ground-based site, although at an altitude of ∼4000 m, so advantageous for photometry. On this basis, longer integrations with a >1 m telescope from similar locations would approach μmag accuracy data for brighter stars. Analysis of eclipsing binary light curves with such an accuracy should allow sensitive tests of theoretical results on stars, and, for the present context, the opacity of stellar material

5. Discussion and Summary

The present study supports the point that changes in schemes for carrying out the numerical integration of structure equations, say of order a few per cent, may have as great, or greater, effect then some of the earlier changes to opacity tables (see also [44]). On the face of it, this looks at variance with the implication of opacity model predictions, testable, in principle, to very high accuracy when suitable observational material is available. Parameters thought to be within $\sim 10^{-4}$ of their real values have been specified [45], but this was when a detailed vibration spectrum also was known. In general, information about stars obtained from direct measurement is less specific: but a useful broad range of data comes from eclipsing binary stars with double-lined spectra, to which the present article is closely related.

Our main findings concern the increase of radius associated with increasing envelope opacity. In this study, changes from the earlier LAOL opacity tables to later ones that include more detailed line absorption effects, have changed calculated radii by up to ∼5–10%. This scale of effect in the radius is now able to be checked by careful analysis of good observations of eclipsing binary stars, even taking into account the interdependence of parameters in the fitting of their light curves. In this way, detailed atomic modelling becomes open to empirical testing from observations. It is interesting that the small difference between the older Iglesias and Rogers opacities and the observations in Figure 1 of Stothers and Chin [32] is about the same as the difference between the effects of opacity from the 1992 to the 1996 OPAL opacities (including more line absorption effects). However, alternative possibilities exist that can also account for changes of this order, in particular the role of convective 'overshooting' [46–48, 21].

On this point, Claret and Gimenez [34, 49] showed that a moderate core overshoot improves the comparison between theoretical apsidal motion constants and observational data. Results for the structural constant (a weighted average of both stars) coming from analysis of apsidal motions observed in certain close binary systems with eccentric orbits were often found to be too large in earlier studies, implying that observed mean radii were greater than predicted by models. But here it should be noted that the radii in the relevant formulae are raised to the fifth power. A 2% error of estimation in the radius would therefore become a 10% error in the estimation of the mean structural constant. This should render the mean structural constant too insensitive to test opacity models on the basis of, say, the Andersen [20] criteria. The role of the most appropriate dynamically stable mean rotation rate for the stars in such eccentric binaries is also likely to be underestimated if the mean orbital angular velocity were used [50]. Light curve analysis models also have often referred to 'Roche model' configurations for the stars, (for example with the Wilson-Devinney 1972 code, or its later developments). But, strictly speaking, there is no 'Roche model' for an eccentric binary system, a point stressed already by [51]. Such comments aside, there will remain the issue of whether any model of a continuum of heat-flow related variables can be uniquely established by observables dependent only on the integrals of such variables.

We note some limitations about the generality of our findings: (a) the role of numerical accuracy effects in the calculations (particularly where there have been some discontinuities in tailoring the Kurucz envelope opacities into the general run of values throughout the star (cf. Figure 4c); and (b) the application of the changed opacities only in the GOB program. In addition to opacity-related effects the GOB+SCH program results show some small effects associated with the location of the internal fitting point and also the adopted convective mixing-length parameter 'alpha'. Nevertheless, we contend that more recent opacities, including fuller treatment of line absorptions, produce effects that can be discriminated from detailed analysis of double-lined eclipsing binary systems observed with modern, high-quality facilities.

References

[1] Kurucz 1998. http://cfaku5.cfa.harvard.edu/opacities/Rosseland/kamp02.ross.

[2] W. F. Huebner, A. L. Merts, N. H. Magee, and M.F. Argo, Los Alamos Scientific Report LA-6760-M.(1977).

[3] C. A. Iglesias and F. J. Rogers, *ApJ*, **371**, (1991), 408.

[4] F. J. Rogers and C. A. Iglesias, *ApJS*, **79**, (1992), 507.

[5] C. A. Iglesias and F. J. Rogers, *ApJ*, **464**, (1996), 943.

[6] M. Schwarzschild, Structure and Evolution of the Stars,*Princeton University Press*, (New Jersey, 1958).

[7] T. R. Carson,*A&AS*, **75**, (1988), 385.

[8] B. Strömgren, mrs.conf.(1967), 461.

[9] D. Prialnik, An Introduction to the Theory of Stellar Structure and Evolution,*Cambridge University Press*, (United Kingdom, 1999).

[10] L. Mestel, *Proc.Camb. Philos. Soc.*, **46**, (1950), 331.

[11] T. R. Carson, *ARA&A*, **14**, (1976), 95.

[12] A. N. Cox and J. N. Stewart, *ApJ*, **19**, (1969), 174.

[13] B. Paczynski, *Acta Astron.*, **2**, (1970), 20.

[14] G. Inlek, A. Böke, O. Yilmaz, E. Budding, *New Astronomy*, **12**, (2006), 427.

[15] P. A. Young, E. E. Mamajek, D. Arnett, J. Liebert, *ApJ*, **556**, (2001), 230.

[16] E. F. Guinan and S. G. Engle, *Ap Space Sci*, **304**, (2006), 5.

[17] D. J. Sullivan and T. Sullivan,*BaltA*, **12**, (2003), 145.

[18] D. M. Popper, H. E. Jorgensen, D. C. Morton and D. S. Leckrane, *ApJ*, **161**, (1970), 57.

[19] J. Andersen, J. V. Clausen, B. Nortdström, J. Tomkin and M. Mayor, *A&A*, **246**, (1991), 99.

[20] J. Andersen, *ASP Conference Series*, **40**, (1993), 347.

[21] A. Claret, *A&A*, **475**, (2007), 1019.

[22] R. B. Stothers and N. R. Simon, *ApJ*, **160**, (1970), 1019.

[23] R. B. Stothers, *ApJ*, **383**, (1991), 820.

[24] M. Loudon, E. Budding, *SouSt*, **37**, (1996), 17.

[25] A. P. Odell, W. D. Pesnell, *ASPC*, **135**, (1998), 69.

[26] R. L. Kurucz, *ASPC*, **108**, (1996), 160.

[27] R. L. Kurucz, *ASPC*, **44**, (1993), 87.

[28] E. Anders, N. Grevesse,*Geochim.Cosmochim.Acta*, **53**, (1989), 197.

[29] W. B. Somerville, *ApJ*, **139**, (1964), 192.

[30] A. Dalgarno, D. A. Williams, *ApJ*, **136**, (1962), 690.

[31] R. B. Stothers, *ApJ*, **194**, (1974), 695.

[32] R. B. Stothers and C. W. Chin, *ApJ*, **381**, (1991), 67.

[33] A. Maeder, G. Meynet, *A&A*, **76**, (1988), 411.

[34] A. Claret and A. Gimenez,*A&AS*, **91**, (1991), 217.

[35] W. A. Dziembowski, IAU Symp, **162**, (1994), 55.

[36] H. N. Russell, Centennial Symposia, Harward Observatory Monographs, Cambridge, MA., **7**, (1948), 181.

[37] S. Jha, D. Charbonneau, P. M. Garnavich, D. J. Sullivan, T. Sullivan, T. M. Brown and J. L. Tonry, *ApJ*, **540**, (2000), 45.

[38] D. Charbonneau, T. M. Brown, D. W. Latham and M. Mayor, *ApJ*, **529**, (2000), 45.

[39] E. Budding, *Ap&SS*, **296**, (2005), 17.

[40] E. Budding and O. Demircan, Introduction to Astronomical Photometry,*Cambridge University Press*, **6**, (Cambridge 2007), 434.

[41] T. Banks and E. Budding, *Ap&SS*, **167**, (1990), 221.

[42] G. W. Henry, G. W. Marcy, R. P. Butler and S. S. Vogt, *ApJ*, **529**, (2000), 41.

[43] T. M. Brown, D. Charbonneau, R. L. Gilliland, N. R. Noyes, A. Burrows, *ApJ*, **552**, (2001), 699.

[44] P. Morel, J. Provost and G. Berthomıeu, *SoPh*, **128**, (1990), 7.

[45] J. Christensen-Dalsgaard, *ESASP*, **286**, (1988), 431.

[46] G. Schaller, D. Schaerer, G. Meynet, A. Maeder, *A&AS*, **96**, (1992), 269.

[47] A. Bressan, F. Fagotto, G. Bertelli, C. Chiosi, *A&AS*, **100**, (1993), 647.

[48] A. Claret, *A&AS*, **109**, (1995), 441.

[49] A. Claret and A. Gimenez, *ASPC*, **40**, (1993), 469.

[50] M. E. Alexander, *Ap.Space Sci*, **23**, (1973), 459.

[51] C. A. Tout, Eggleton, *ApJ*, **334**, (1988), 357.